On the oscillatory dynamical behaviour of epidemic spreading in fractal media

2008 J. Phys. A: Math. Theor. 41 045001

(http://iopscience.iop.org/1751-8121/41/4/045001)

IOP PUBLISHING JOURNAL OF PHYSICS A: MATHEMATICAL AND THEORETICAL

J. Phys. A: Math. Theor. **41** (2008) 045001 (11pp) doi:10.1088/1751-8113/41/4/045001

On the oscillatory dynamical behaviour of epidemic spreading in fractal media

M A Bab and E V Albano

Instituto de Investigaciones Fisicoquímicas Teóricas y Aplicadas (INIFTA), Facultad de Ciencias Exactas, UNLP, CONICET, Casilla de Correo 16, Sucursal 4, (1900) La Plata, Argentina

E-mail: ealbano@inifta.unlp.edu.ar

Received 9 October 2007, in final form 29 November 2007
Published 15 January 2008
Online at stacks.iop.org/JPhysA/41/045001

Abstract

We present numerical evidence that dynamical physical processes that develop a time-dependent characteristic length, and take place in fractal media exhibiting spatial discrete scale invariance (DSI) with fundamental scaling ratio b, may become coupled to the topology of the fractal leading to the observation of time DSI. The hallmark of time DSI is the observation of a log-periodic modulation of the dynamic or kinetic observables, which is characterized by a well-defined fundamental time scaling ratio (τ). Both fundamental scaling ratios are linked according to $b = \tau^{1/z}$, where z is the dynamic exponent characteristic of the physical process. Specifically, we have studied the epidemic behaviour of the contact process (CP) in Sierpinski Carpets. The CP exhibits second-order irreversible phase transitions between an active regime and an absorbing state where the system is trapped without any escape possibility. We observed that relevant dynamic observables, such as the number of active sites, the survival probability of the epidemics and the mean square displacement of the epidemic from the origin ($R^2(t)$), exhibit log-periodic modulations. By fitting the data we evaluate the fundamental time scaling ratio for various fractals and the corresponding dynamic exponents. Since, at criticality, one has that $R^2(t) \propto t^{2/z}$, an independent estimation of the dynamic exponent can be performed, in excellent agreement with results obtained by using the conjectured relationship for the fundamental scaling ratios b and τ.

PACS numbers: 64.60.Ht, 02.50.Ey, 05.50.+q, 05.10.Ln

1. Introduction

The study of far-from equilibrium processes and systems is a topic of interdisciplinary research that even nowadays possesses a formidable challenge [1, 2]. Within this broad context, considerable attention has recently been drawn to the study of irreversible phase transitions

(IPTs) that take place between an active—fluctuating—state and an absorbing state where the activity stops, i.e. a configuration that can be reached by the dynamics but cannot be left [3–7]. The occurrence of IPTs has been reported in a great variety of models including, among others, directed percolation [3–6], catalytic reactions [5–7], forest-fire models [8], branching annihilating random walkers with an odd number of offsprings [9], epidemic spreading without immunisation [10], prey–predator systems [11], the Domany–Kinzel cellular automata [12], the contact process [3–6], etc (for reviews see [4–7]).

Continuous second-order IPTs share many characteristics with their equilibrium counterparts. In fact, they exhibit a diverging correlation length when the control parameter approaches criticality. Consequently, relevant observables exhibit scale-invariance and obey power-law functions with well-defined exponents. These exponents can be grouped into sets that define universality classes [4–7]. So far, the most ubiquitous universality class for IPTs is directed percolation [5, 6]. By taking advantage of the existence of a diverging correlation length, a finite-size scaling theory, conceptually similar to that used for the description of equilibrium transitions [13], can be formulated for the study of IPTs by means of numerical simulations [5]. However, as the critical point is approached and fluctuations become enhanced, the system may irreversibly fall into the absorbing state—even for values of the control parameter laying within the active regime—hindering the clean application of the finite-size scaling approach. This shortcoming can be overcome by performing a special kind of dynamic measurement generically called epidemic studies [14]. The idea behind the epidemic approach is to initialize the simulation by using a configuration very close to the absorbing state. For this purpose one actually starts with the absorbing state slightly modified by removing (adding) few particles from (to) a place close to the centre of the sample, when such a state is a fully occupied (vacuum) one. Subsequently, the system is allowed to evolve according to the particular rules of the model under consideration. During this dynamic process the following quantities are recorded: (i) the average number of empty (occupied) sites $N(t)$ for fully occupied (vacuum) absorbing states, (ii) the survival probability $P(t)$, which is the probability that the epidemic is still active at time t, and (iii) the average mean square distance, $R^2(t)$, over which the epidemic has spread. It is worth mentioning that each single epidemic stops if the sample becomes trapped in the absorbing state, so that results have to be averaged over many different epidemics. Also, note that $N(t)$ ($R^2(t)$) is averaged over all (surviving) epidemics.

By performing the epidemic close to the critical point (p_c) of a second-order IPT, say at a generic distance ϵ, power-law behaviour due to scale invariance can be assumed and the following Ansatzen are expected to hold:

$$N(t) \propto t^{\eta} N^*(\epsilon t^{1/\nu_\parallel}), \tag{1}$$

$$P(t) \propto t^{-\delta} P^*(\epsilon t^{1/\nu_\parallel}), \tag{2}$$

and

$$R^2(t) \propto t^{z_e} R^*(\epsilon t^{1/\nu_\parallel}), \tag{3}$$

where η, δ and z_e[1] are dynamical critical exponents, $\nu_\parallel$ is the correlation length exponent in the time (growing) direction, and N^*, P^* and R^* are scaling functions [14]. Thus, at the critical point one has $\epsilon = 0$ and the scaling functions adopt constant values, so log-log plots of $N(t)$, $P(t)$ and $R^2(t)$ will asymptotically show straight-line behaviour, while off-critical points will exhibit a curvature. By taking advantage of this behaviour one can evaluate quite

[1] We identify z_e as the dynamic epidemic exponent, which may be different from the standard dynamic exponent (z) that is used in the study of second-order transitions.

accurately both the critical point and the dynamic exponents [14]. It should be noted that by preventing the epidemic to reach the boundary of the sample one obtains critical values free of undesired finite-size effects.

IPTs have been studied not only in regular lattices [4–7], but also in some fractals [5] such as Sierpinski Carpets [15–18], percolation clusters [19, 20], diffusion limited aggregates [21], etc. In fact, for some physical situations a regular lattice may not be appropriate to give a realistic description of the underlying media where the physical process actually takes place, e.g. for a catalytical reaction in a fractal catalyst, the propagation of a disease in a complex network, etc. Focusing our attention to the dynamic behaviour of IPTs in fractal media—more specifically in the epidemic behaviour—it should be expected that under appropriated conditions, e.g. when the fractal exhibits discrete scale invariance (DSI) [22], the dynamical evolution of some observables may become somewhat coupled to some topological property of the underlying substrata. In fact, DSI is a weak kind of scale invariance such that an observable $O(x)$, which is a function of a control parameter x, obeys the scaling law

$$O(x) = \mu(b)O(bx), \tag{4}$$

under the change $x \to bx$. Here b is no longer an arbitrary real number, as in the case of *continuous* scale invariance, but it can only take specific discrete values of the form $b_n = (b_1)^n$, where b_1 is a fundamental scaling ratio. If an observable $O(x)$ satisfies equation (4) for an arbitrary b, it necessarily has to obey a power law of the type $O(x) = Cx^\alpha$, where α is an exponent. But in the case of DSI, the solution of equation (4) yields

$$O(x) = x^\alpha F\left(\frac{\log(x)}{\log(b_1)}\right), \tag{5}$$

where F is a periodic function of period one.

Within this context, the purpose of this paper is to develop a conjecture linking the spatial DSI of fractals with the observation of time DSI in dynamic observable of physical phenomena occurring on these media. Time DSI would become evident by the occurrence of the log-periodic modulation of the dynamic or kinetic observable exhibiting power-law behaviour, similar to the case of equation (5) but in the time domain. Furthermore, we will test the conjecture by means of extensive computer simulations analysed with the aid of scaling arguments. For this purpose we have chosen to study the epidemic behaviour of the contact process (CP) [3, 23] in Sierpinski Carpets of different fractal dimensions. The CP is an archetypical example of interacting particle systems exhibiting IPTs [3].

It is worth mentioning that the interplay between the spatial DSI and the kinetics of random walks leads to the occurrence of log-periodic oscillations in the return probabilities, as has first been demonstrated analytically by Grabner and Woess [24] for the case of fully symmetric Sierpinski gaskets. They evidenced the oscillation phenomena by applying a technique early developed by Flajolet and Odlyzko [25] studying the singularity of the Green function at $z = 1$. These results have then been extended by Krön and Teufl [26] to a large class of mathematical fractals (cell graphs) where some more details on the application of the technique based on the singularities in Green functions can be found, together with additional mathematical literature on these topics. Furthermore, we have shown [27], by means of numerical simulations, that the oscillatory behaviour becomes also evident in the number of distinct sites visited by the random walk, as well as in diffusion-controlled reactions among walkers occurring in fractal media exhibiting spatial DSI.

The paper is organized as follows: in section 2, we provide the definition of the contact process and give a brief description of the simulation method. The main characteristics of the used fractals are also presented in section 2. Section 3 is devoted to the discussion of the

concept of DSI while our results are presented and discussed in section 4. Finally, we state our conclusions in section 5.

2. The contact process on fractal media and the simulation method

The contact process (CP), originally introduced by Harris [23], is a simple model for the spread of epidemics through a network or lattice. The network, usually taken to be a hyper-cubic lattice, the nodes or sites can be in one of the two states: 'infected' (occupied, $(\sigma_i(t) = 1)$) or 'susceptible' (vacant $\sigma_i(t) = 0$). Transitions from $\sigma_i = 1$ to $\sigma_i = 0$ occur spontaneously with probability λ, independent of the neighbouring sites. On the other hand, the reverse transition, from $\sigma_i = 0$ to $\sigma_i = 1$, takes place with probability $1 - \lambda$. In this case an occupied site creates autocatalytically a new one, in a randomly selected vacant nearest-neighbour site. Thus the state $\sigma_i = 0$ for all i is absorbing and, in all dimensions, the CP undergoes a continuous (second-order) IPT into an absorbing state such as the system becomes trapped into the vacuum state. Also, λ is a control parameter governing the rate of spreading of the activity and λ_c is the critical point for the IPT.

Although no exact results are available, the CP has been studied intensively via series expansion [3, 4, 28] and Monte Carlo simulations [3–6, 29]. The model has attracted much interest as a prototype of a nonequilibrium critical point, a simple representative of the directed percolation (DP) universality class and its scaling properties have been discussed extensively [4–6].

In this paper, the CP is studied in Sierpinski Carpets, which are built up by segmenting a square in b^2 subsquares and removing c^2 of them from the centre ($SC(b, c)$). This segmentation process is iterated in the remaining subsquares a number k of steps, and the mathematical fractal is obtained after an infinite number of segmentation steps. Nevertheless, in order to perform the simulations one has to use a finite segmentation step, which has to be large enough for the observables to become almost independent of k. On the other hand, by increasing b and c it is possible to decrease the fractal dimension of the $SC(b, c)$, which is given by $d_f = \frac{\log(b^2-c^2)}{\log b}$. In this way one also increases the size of the holes in the structure, and one then says that the lacunarity is larger. As a consequence of the described iterative process, the topological details of the generating cell are present in any scale, and then the structure is scale invariant only for a well-defined spatial scaling ratio b.

3. Spatial and temporal discrete scale invariance

In order to develop a preliminary argument, let us recall that a typical average size of an epidemic (ξ) obeys the following relationship,

$$\xi \propto t^{1/z}, \tag{6}$$

where z is the dynamic exponent linking space and time, as used within the context of standard second-order transitions (see footnote 1). It should be noted that z differs from the dynamic spreading exponent z_e defined in the context of equation (3), but by comparing equations (3) and (6) it can easily be shown that both exponents are linked, such that $z_e = 2/z$.

Now, let us consider those fractals obeying discrete scale invariance [22] and consequently exhibiting log-periodic oscillations of some observables as a function of the distance to a given point (see equation (5)), e.g. the number of sites of the fractal within a circle of a given radius, as shown in figure 1 for the fractals used in this paper. The insets, which clearly show the shape of the oscillations, are obtained by plotting the number of sites of the fractal, already shown in the main panel, but after subtracting and normalising the data by πR^{d_f} versus R,

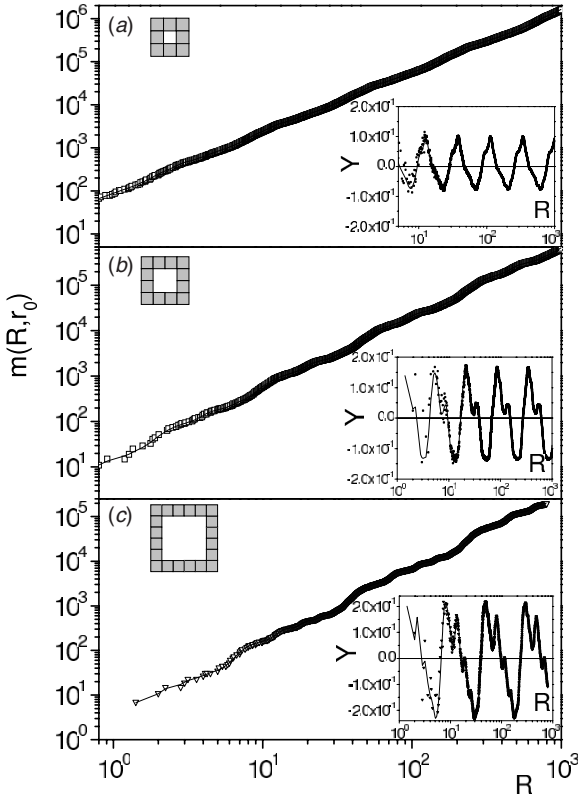

Figure 1. Log–log plot of the number of fractal sites within a circle of given radii $m(R, \mathbf{r_0})$, as obtained for the fractals whose generating cell is shown in the upper-left corner of the corresponding figure. The insets show linear–log plots of $Y = \frac{m(R,\mathbf{r_0})-\pi R^{d_f}}{\pi R^{d_f}}$ versus R, which allow a clear observation of the oscillations. More details are given in the text.

in linear-log scale. In all these cases, one has that the oscillations are characterized by a well-defined scaling ratio (b). So, if the epidemic is somewhat coupled to the topology of the fractal, one may observe temporal log-periodic oscillations in the dynamic observables with a well-defined time scaling ratio (τ). By making the conjecture that a dynamic observable, written in terms of ξ as given by equation (6), obeys DSI [27], then τ becomes properly coupled to the spatial scaling ratio, namely

$$b = \tau^{1/z}. \tag{7}$$

Of course, the detection of soft oscillations in epidemic simulations possesses a difficult challenge since huge statistics for large simulation times are expected to be necessary. In fact, in early simulation results of both the contact process [16] and the catalytic oxidation of carbon monoxide [30] (i.e. the ZGB model) we are unable to detect evidence of oscillations in the reported data. However, a careful inspection of figures 2(b) and 3(b) of the paper of Gao *et al* [31] suggests the presence of soft oscillations in the dynamic behaviour of $N(t)$ for the simulation of the ZGB model at criticality. This observation is possible due to the noticeable statistics used (averages one taken over 10^6 to 2×10^6 different runs), in spite of the fact that short measurement times (2×10^3) are considered.

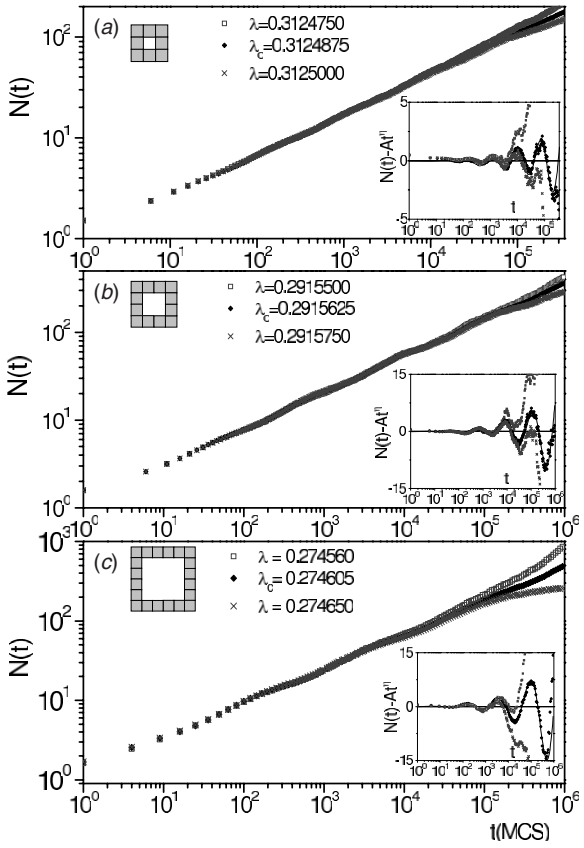

Figure 2. (*a*)–(*c*) Log–log plots of the number of active sites ($N(t)$) versus time, as obtained for different fractals whose generating cell is shown in the upper-left corner of the corresponding figure. In all the cases a supercritical, a critical and a subcritical epidemic are shown. The insets show, in a linear–log plot, the time dependence of the results shown in the main panel modified after subtracting the modulated power-law fit of the data. Results obtained by fitting the numerical data by using equation (8) are listed in table 1. More details are given in the text.

4. Results and discussion

Figures 2(*a*)–(*c*) show log–log plots of the number of active sites ($N(t)$) as a function of t, obtained for different values of the control parameter λ and various fractal substrates (the generating cell of the corresponding fractal is shown in each figure). In all the cases epidemics are started by placing a single active site close to the centre of the fractal in an otherwise vacuum state. For each fractal we have shown the results obtained for three different epidemics performed close to the critical point (many other epidemics performed in order to approach criticality are not shown for the sake of clarity). A careful inspection of figure 2(*a*) reveals the presence of soft oscillations of the epidemics performed in the $SC(3, 1)$. These oscillations become more evident when the fractal dimension (lacunarity) is decreased (increased), as follows from figures 2(*b*) and (*c*) corresponding to the $SC(4, 2)$ and $SC(6, 4)$, respectively. On view of these results and within the context of the already performed discussion on the interplay between spatial and time DSI, we have fitted the data to a power-law divergence

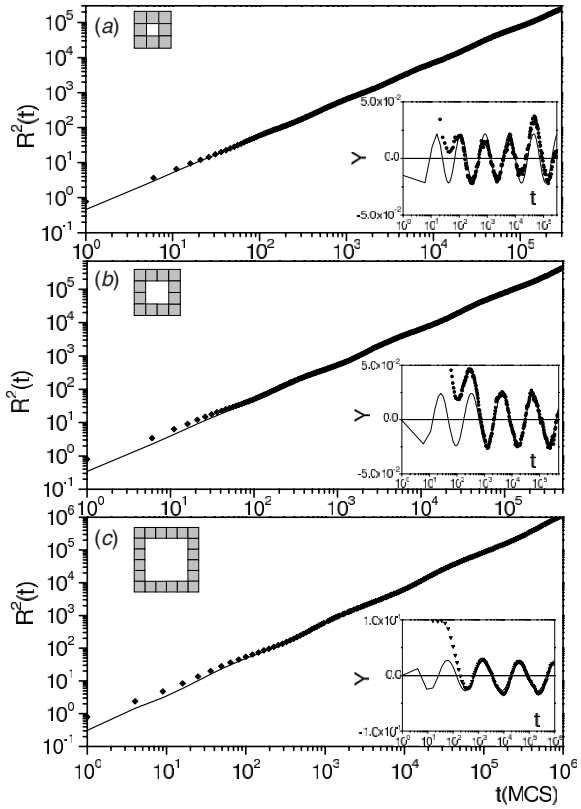

Figure 3. (*a*)–(*c*). Log–log plots of $R^2(t)$) versus time, as obtained at criticality for different fractals whose generating cell is shown in the upper-left corner of the corresponding figure. The insets show linear–log plots of the time dependence of $Y = \frac{R^2(t)-At^{z_e}}{At^{z_e}}$. Results obtained by fitting the numerical data are listed in table 1. More details are given in the text.

modulated by a log-periodic function given by,

$$N(t) = At^{\eta}(1 + B\cos(2\pi \log(t)/\log(\tau) + \phi)), \tag{8}$$

where η is an exponent, $\log(\tau)$ is the logarithmic period and ϕ is the phase constant. Also, A and B are constants. After obtaining the best fits of the data (a summary of the obtained results is shown in table 1) we proceed to decouple the modulation just by subtracting the power law to the measured value of $N(t)$, as shown in the insets of figures 2(*a*)–(*c*). By using this procedure the oscillatory behaviour becomes clear beyond any doubt even for the fractal of lower lacunarity, namely the $SC(3, 1)$ as shown in figure 2(*a*). It is worth mentioning that this subtracting procedure also allows us to obtain a quite accurate determination of the critical point because noticeable upward (downward) deviations of the oscillatory behaviour are observed when the values of the control parameter are within the active (absorbing) phase of the system, see the insets of figures 2(*a*)–(*c*).

On the other hand, figures 3(*a*)–(*c*) show log–log plots of $R^2(t)$ versus t as obtained at criticality for the fractals $SC(3, 1)$, $SC(4, 2)$ and $SC(6, 4)$, respectively. In all the cases one observes soft log–periodic oscillations that can easily be observed in linear–log plots of $Y = \frac{R^2(t)-At^{z_e}}{At^{z_e}}$ versus time, as show in the insets of the corresponding figures.

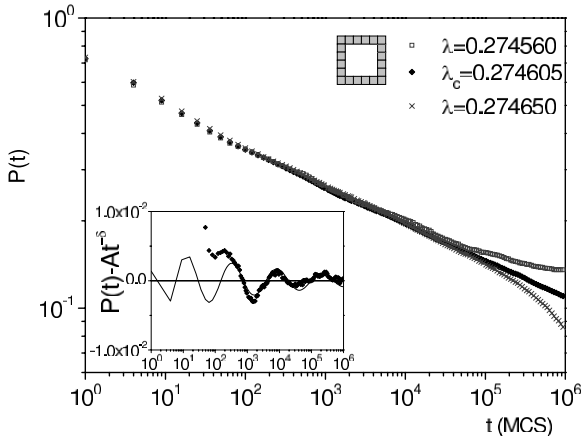

Figure 4. Log–log plots of the survival probability of the epidemics $P(t)$) versus time, as obtained for three different values of the control parameter close to criticality and for the $SC(6, 4)$ whose generating cell is shown in the upper-left corner of the figure. The inset shows in a linear–log scale, the time dependence of the results, obtained at criticality, shown in the main panel modified after subtracting the modulated power-law fit of the data. Results obtained by fitting the numerical data are listed in table 1. More details are given in the text.

Table 1. Critical exponents and logarithmic periods obtained by fitting the measured data, corresponding to different fractals, and for the following observables: (i) number of active sites (second and third columns), (ii) the mean square displacement of the epidemics from the origin (fourth and fifth columns) and (iii) the survival probability of the epidemics (sixth and seventh columns). More details are given in the text.

SC$(b, c), k, L$	η	$\log(\tau)$	z_e	$\log(\tau)$	δ	$\log(\tau)$
(3,1), 7, 2187	0.406(2)	0.882(9)	1.047(7)	0.873(18)	0.211(8)	–
(4,2), 6, 4096	0.415(2)	1.122(4)	1.071(3)	1.12(2)	0.166(4)	1.18(5)
(6,4), 5, 7776	0.432(3)	1.415(16)	1.090(3)	1.42(2)	0.126(4)	1.41(3)

We also found that the time behaviour of the survival probability of the epidemics (see equation (2)) is less sensitive to the underlying structure of the fractal. In spite of this shortcoming we are still able to decouple the oscillations as shown in figure 4 for the case of the $SC(6, 4)$.

Results corresponding to the best fits of the data obtained by using equation (8) (and the corresponding functions for $P(t)$ and $R^2(t)$), for the three different fractals studied are summarized in table 1. We found that—within error bars—the period of the oscillation is independent of the observable used for its calculation—either $N(t)$, $P(t)$ and $R^2(t)$—further supporting the procedures used to fit the numerical results. It is also worth mentioning that the measurements of $R^2(t)$ provide a very useful alternative test for the conjecture outlined in section 3. In fact, according to equations (3) and (6), the exponent z_e and the dynamic exponent z are linked through $z_e = 2/z$. On the other hand, the spatial scaling ratio of the fractal is also linked to the time scaling ratio of the dynamic process evolving on the fractal (see equation (7)). Thus, the exponents determined by using equations (3) and (7) are summarized in table 2. The excellent agreement obtained by comparing the two independent determinations of the dynamical exponent, and for the three different fractals studied, strongly supports the outlined conjecture linking the dynamic oscillations of the physical process to geometrical properties of the underlying media where the process actually takes place.

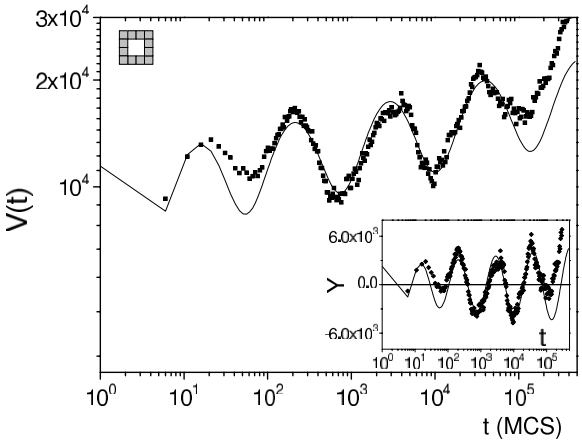

Figure 5. Log–log plots of the logarithmic derivative of the number of active sites versus time, as obtained for the $SC(4, 2)$ whose generating cell is shown in the upper-left corner of the figure. The inset shows a linear–log plot of $Y = \frac{V(t)-At^{1/\nu_\parallel}}{At^{1/\nu_\parallel}}$ as function of time.

Table 2. Dynamical exponents (z) (third column) obtained with the aid of the conjectured equation (7) by using the fundamental (spatial) scaling ratio of each fractal (first column) and the logarithmic period measured by fitting the oscillations of different physical observables (second column). For the sake of comparison, independent evaluations of the dynamic exponent as obtained by measuring the mean square displacement of the epidemics from the origin are listed in the fourth column. More details are given in the text.

Fractal	Observable	z	$2/z_e$
$SC(3, 1)$	$N(t)$	1.85(2)	
$d_f = 1.8927$	$R^2(t)$	1.84(5)	1.91(2)
$SC(4, 2)$	$N(t)$	1.863(7)	
$d_f = 1.7925$	$P(t)$	1.96(8)	
	$R^2(t)$	1.86(3)	1.867(5)
$SC(6, 4)$	$N(t)$	1.82(2)	
$d_f = 1.7227$	$P(t)$	1.81(4)	
	$R^2(t)$	1.83(2)	1.835(5)

So far, we have discussed results obtained at criticality. However, it is known that off-criticality the Ansatz given by equation (1) can be used in order to compute the logarithmic derivative, so that one obtains

$$V(t) = \left.\frac{\partial \ln N(t)}{\partial t}\right|_{(\epsilon\equiv 0)} \propto t^{1/\nu_\parallel} \tag{9}$$

that evaluated at criticality ($\epsilon = 0$) allows the determination of the exponent $1/\nu_\parallel$ by means of a suitable fit of the data. The numerical calculation of the log derivative given by equation (9) is quite demanding because one needs to have, at least, three well-averaged epidemics (one at criticality and the remaining ones slightly off-criticality). However, as shown in figure 5 for the case of the $SC(4, 2)$, we have achieved enough statistics in order to show a reliable log–log plot of the logarithmic derivative versus t. Also, figure 5 clearly shows a well-defined oscillatory behaviour with a logarithmic period $\log(\tau) = 1.14(2)$, which yields $z = 1.89(3)$ in excellent agreement with the values obtained at criticality (see table 1).

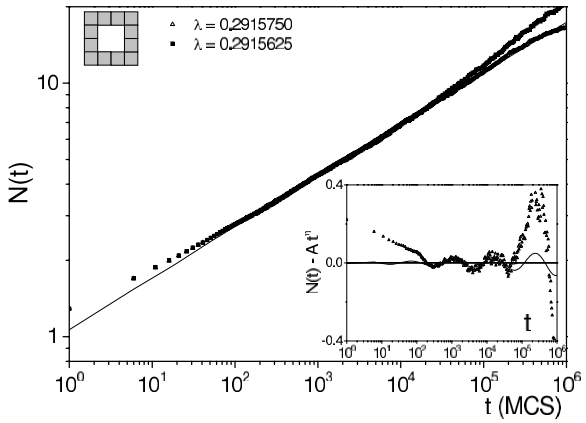

Figure 6. Log–log plots of the number of active sites ($N(t)$) versus time, obtained close to criticality, for epidemics launched at randomly chosen sites in the $SC(16, 4)$. The inset shows ($N(t)$) versus time, after subtracting the modulated power-law, for $\lambda = 0.291\,5750$. More details are given in the text.

As already anticipated, all the results discussed above have been obtained by starting the epidemics from a site close to the geometrical centre of the fractal. In this way, one avoids the statistical interference among epidemics having different phase constants (ϕ in equation (8)) that is expected to occur for different initial conditions. In fact, we observed that by averaging epidemics started from different—random selected—sites of the fractal, the oscillations become severely damped. Figure 6 shows a log–log plot of $N(t)$ versus t obtained close to criticality for epidemics launched at randomly chosen sites in the $SC(4, 2)$. One observes that due to the huge statistics—averages are taken over 6×10^5 different epidemics—one can still, but hardly, observe the power-law behaviour modulated by a log-periodic oscillation (see the inset of figure 6). The best fit of the data is achieved with $\log(\tau) = 1.12(6)$, in excellent agreement with the results obtained with epidemics started from a single fixed site (see table 1). This observation points out that the subtle interplay between the dynamics of the physical process and the topology of the fractal, leading to time DSI, requires careful measurements in order to avoid the occurrence of interference effect that may hinder the actual physical behaviour as it would be simply noise.

5. Conclusions

We studied the epidemic behaviour of the contact process in various Sierpinski Carpets, showing that dynamical observables are subtly coupled to the spatial discrete scale invariance of the underlying fractal, leading to the occurrence of time DSI. Time DSI becomes evident by the observation of log-periodic modulations in the power-law behaviour of relevant dynamic observables of the epidemics.

Our numerical results allow us to successfully test the conjecture that both, spatial (b) and time (τ), fundamental scaling ratios are linked according to $b = \tau^{1/z}$, where z is the dynamic exponent characteristic of the physical process. The conjecture is further tested by an independent determination of z performed by measuring the mean square displacement of the epidemic from the origin.

We expected that the occurrence of time DSI in the physical process occurring on fractal media exhibiting spatial DSI is no longer restricted to the random walk [24, 26] and the

irreversible phase transition of the CP, but instead it may be a quite general phenomenon. In fact, apart from our early observation of time DSI in the case of the equilibrium (reversible) phase transition characteristic of the Ising magnet in fractal media [32], our preliminary results also confirm its occurrence in archetypical cases such as annihilation reactions among random walks, coarsening dynamics without surface tension (vorter model) and interfacial behaviour in growing models.

Acknowledgment

This work was supported financially by CONICET, UNLP and ANPCyT (Argentina).

References

[1] Gardiner C W 1990 *Handbook of Stochastic Methods* (Berlin: Springer)
[2] van Kampen N G 1992 *Stochastic Processes in Physics and Chemistry* (Amsterdam: North-Holland)
[3] Liggett T M 1985 *Interacting Particle Systems* (New York: Spinger)
[4] Marro J and Dickman R 1999 *Phase Transitions and Critical Phenomena* (Cambridge: Cambridge University Press)
[5] Hinrichsen H 2000 *Adv. Phys.* **49** 815
Hinrichsen H 2006 *Physica* A **369** 1
[6] Ódor G 2004 *Rev. Mod. Phys.* **76** 663
[7] Loscar E and Albano E V 2003 *Rep. Prog. Phys.* **66** 1343
[8] Albano E V 1994 *J. Phys. A: Math. Gen.* **27** L881
Clar S, Drossel B and Schwalb F 1996 *J. Phys.: Condens. Matter* **8** 6803
[9] Jensen I 1994 *Phys. Rev.* E **50** 3623
Takayasu H and Tretyakov T 1992 *Phys. Rev. Lett.* **68** 3060
Jensen I 1993 *Phys. Rev.* E **47** R1
[10] Gassberger P 1982 *Math. Biosci.* **63** 157
[11] Rozenfeld A F and Albano E V 2001 *Phys. Rev.* E **63** 061907
[12] Domany E and Kinzel W 1984 *Phys. Rev. Lett.* **53** 311
[13] Landau D P and Binder K 2000 *A Guide to Monte Carlo Simulations in Statistical Physics* (Cambridge: Cambridge University Press)
[14] Grassberger P and de la Torre A 1979 *Ann. Phys. (NY)* **122** 373
Grassberger P 1989 *J. Phys. A: Math. Gen.* **22** 3673
[15] Albano E V 1992 *Phys. Lett.* A **168** 55
[16] Jensen I 1991 *J. Phys. A: Math. Gen.* **24** L1111
[17] Mai J, Casties A and Von Niessen W 1992 *Chem. Phys. Lett.* **196** 358
[18] Tretyakov A Yu and Takayasu H 1991 *Phy. Rev.* A **44** 8388
[19] Albano E V 1990 *Surf. Sci.* **235** 351
Albano E V 1990 *Phys. Rev.* B **42** R10818
[20] Casties A, Mai J and von Niessen W 1993 *J. Chem. Phys.* **99** 3082
[21] Mai J, Casties A and Von Niessen W 1993 *Chem. Phys. Lett.* **221** 197
[22] Sornette D 1998 *Phys. Rep.* **297** 239
[23] Harris T E 1974 *Ann. Prob.* **2** 969
[24] Grabner P J and Woess W 1997 *Stoch. Process. Appl.* **69** 127
[25] Flajolet P and Odlyzko A M 1990 *SIAM J. Discrete Math.* **3** 216
[26] Teufl E 2003 *Combin. Probab. Comput.* **12** 203
Krön B and Teufl E 2004 *Trans. Am. Math. Soc.* **356** 393
[27] Bab M A, Fabricius G and Albano E V 2007 *Preprint* 0708.2222.bab
[28] Jensen I and Dickman R 1994 *Physica* A **203** 175
[29] Jensen I 1992 *Phys. Rev.* A **45** R563
[30] Albano E V 1994 *J. Phys. A: Math. Gen.* **27** 431
[31] Gao Z and Yang Z R 1999 *Phys. Rev.* E **59** 2795
[32] Bab M A, Fabricius G and Albano E V 2006 *Phys. Rev.* E **74** 041123